Optical single-channel recording: imaging Ca^{2+} flux through individual ion channels with high temporal and spatial resolution

Angelo Demuro
Ian Parker
University of California, Irvine
Department of Neurobiology and Behavior
Irvine, California 92697-4550
E-mail: iparker@uci.edu

Abstract. Developments in imaging technology now enable visualization of the functioning of individual ion channels in living cells: something previously possible only by the electrophysiological patch-clamp technique. We review techniques that track channel gating via changes in intracellular [Ca^{2+}] resulting from openings of Ca^{2+}-permeable channels. Spatial and temporal resolution are optimized by monitoring Ca^{2+} close to the channel mouth, and we describe the use of two imaging modalities: confocal laser scan microscopy (linescan CLSM) and total internal reflection fluorescence microscopy (TIRFM). Both currently achieve a kinetic resolution of <10 ms, provide a simultaneous and independent readout from many channels, and enable their locations to be mapped with submicrometer resolution. TIRFM provides 2-D images from a very thin (~100 nm) optical section, but it is restricted to channels in the plasma membrane of cells adhering close to a cover glass. In contrast, CLSM can image channels in intracellular membranes but, to achieve good temporal resolution, has been utilized only in a linescan mode with limited spatial information. We anticipate that imaging techniques will develop as a useful adjunct to patch-clamping for single-channel studies, with capabilities including simultaneous readout from multiple channels, high-resolution mapping of channel location, and mobility that is inaccessible by electrophysiological means. Optical single-channel recording is applicable to diverse voltage- and ligand-gated Ca^{2+}-permeable channels and has potential for high-throughput functional analysis. [DOI: 10.1117/1.1846074]

Keywords: single-channel imaging; total internal reflection microscopy; confocal microscopy; *N*-type Ca^{2+} channels; optical patch clamp.

Paper NEU-01 received Mar. 1, 2004; revised manuscript received Apr. 30, 2004; accepted for publication May 6, 2004; published online Feb. 2, 2005.

1 Introduction

Patch-clamp recording was the first technique capable of monitoring the function of single biological molecules,[1,2] and it has revolutionized studies of ion channels by enabling measurement of single-channel currents with exquisite resolution. In contrast to this electrophysiological approach, most subsequent developments in single molecule studies have utilized optical techniques such as the imaging of individual green fluorescent protein (GFP)-tagged proteins[3] and measurement of molecular motors.[4] Optical techniques also hold promise as alternative methodologies for studying single-ion-channel functioning, with capabilities that cannot be attained by electrophysiological techniques; including simultaneous readout from numerous ion channels and information about ion channel distribution and motility within the cell membrane.

One approach to image the functioning of individual ions channels involves the use of fluorescent reporters sensitive to change in the protein structure.[5] This method has important advantages in that it can provide information regarding conformational changes in channel structure, not merely channel opening, and is, in principle, applicable to virtually all types of channels. However, its utility for single-channel studies is likely to be limited in practice, owing to the weak signals and rapid photodestruction that result because only one or a few fluorophores can be conjugated to each channel.

A very different approach utilizes fluorescent indicator dyes to sense Ca^{2+} ions passing through individual channels.[6–10] This provides an enormous inherent amplification, because thousands of Ca^{2+} ions per millisecond flow through an open channel, and each dye molecule that binds Ca^{2+} can be excited to emit thousands of photons. Moreover, cells maintain their cytosolic resting free Ca^{2+} concentration at very low levels, so that influx of Ca^{2+} through even a single channel results in a large local concentration increase. Several early reports described fluorescence signals that were attributed to openings of single intracellular Ca^{2+} release

1083-3668/2005/$22.00 © 2005 SPIE

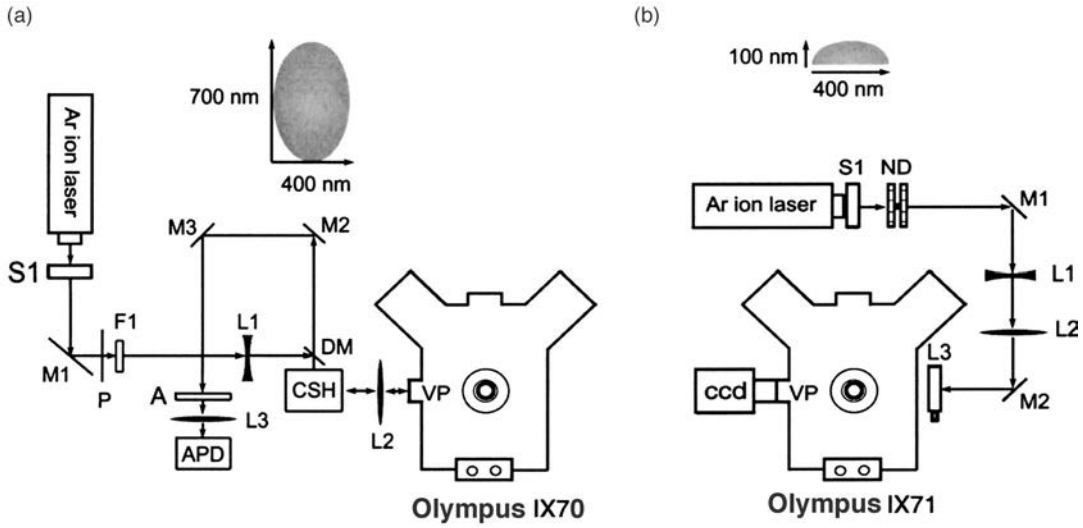

Fig. 1 Confocal linescan and total internal reflection fluorescence microscopy (TIRFM) systems for single channel imaging. (a) Schematic layout of the linescan confocal microscope. A custom-built scanner is interfaced through the side (video) port (VP) of an Olympus IX70 microscope equipped with an oil-immersion 40× objective lens [numerical aperture (NA)=1.35]. Light from an argon ion laser is attenuated by a rotating polarizer (P), filtered (F1) to select the 488-nm line, diverged by lens L1 (f= 200 mm) and directed onto a scan mirror (CSH) via a dichroic mirror (DM) reflecting λ<500 nm. Lens L2 is a scan lens (10× ocular) that focuses the beam as a spot in the specimen, the position of which moves linearly with rotation of the scan mirror. Emitted fluorescence is collected by the objective lens, is descanned and detected by an avalanche photodiode (APD) photon-counting module after passing through a barrier filter, confocal aperture (A) and collimating lens (L3). Mirrors (M1 through M3) are fully reflecting front surface mirrors; S1 is an electronic shutter. The inset diagram illustrates the dimensions of the diffraction-limited confocal spot in the x and z dimensions. (b) Schematic of the TIRFM. This is based around an Olympus IX 71 microscope equipped with an Olympus 60× TIRFM objective (NA=1.45). Excitation light from an argon ion laser (488 nm) is attenuated by a neutral density attenuator (ND), expanded by a telescope formed from lenses L1 and L2 and brought to a focus at the rear focal plane of the objective by L3. Translation of L3 enables the beam to be introduced either at the extreme edge of the objective aperture (for TIR excitation), or more centrally (for "wide-field") excitation. Laser light is directed into the objective by a dichroic mirror (λ=500 nm) in the epifluorescence turret, and emitted fluorescence is collected through the objective, dichroic and a barrier filter (>510 nm). Fluorescence signals are imaged using an intensified video-rate CCD camera, or a fast, cooled CCD camera with on-chip electron multiplication (Cascade, Roper Scientific). The inset diagram shows the point spread function obtained with TIRFM imaging, and illustrates the improved axial resolution as compared to confocal imaging.

channels.[11–14] However, the first unequivocal demonstrations of single-channel fluorescence signals were provided by Zou et al.[6] and Wang et al.,[8] who combined imaging and electrophysiological techniques to record Ca^{2+} signals simultaneously with current flow through individual plasma membrane channels.

Two divergent methods have been used to image single-channel Ca^{2+} signals.[15] Zhou et al.[6,7] used high-speed, wide-field fluorescence microscopy to image Ca^{2+} influx through sparsely distributed membrane channels. By summing the fluorescence over a large volume of the cell they obtained a measure of the fluorescence "signal mass,"[16] which reflects an integral of Ca^{2+} flux throughout the duration of a channel opening. The rate of rise of signal mass thus provides a good measure of the underlying Ca^{2+} current, and is essentially independent of whether or not the transient is in focus.[6] Moreover, local fluorescence measurements obtained at the center of the event track channel gating with a time resolution of a few tens of milliseconds: that is, the fluorescence rose and decayed with a half time of about 25 ms following channel openings and closings.[7] The alternative approach involves using optical sectioning techniques, including confocal microscopy[8,9] and total internal fluorescence microscopy,[10] to monitor fluorescence signals from subfemtoliter volumes immediately around the channel mouth. In principle, this should provide a better kinetic resolution and separation of closely adjacent signals than is possible by wide-field imaging, because of the precipitous Ca^{2+} gradients (microdomains) that exist around an open Ca^{2+} channel. Ca^{2+} concentrations of greater than 100 μM are likely at the channel mouth, but the concentration falls to <1 μM at distances of only about 1 μm.[17,18] Furthermore, whereas the local Ca^{2+} concentration at the channel mouth rises and falls almost instantly as the channel opens and closes, these changes slow quadratically as a function of distance from the channel mouth. Measurements restricted to the immediate vicinity of a channel are thus expected to track its gating more faithfully than wide-field images in which out-of-focus fluorescence from distant regions will "dilute" and slow the signal.

In the following sections we review recent efforts in our laboratory to develop improved methods for imaging single-channel activity via Ca^{2+} flux through the channels.[9,10] Our aims are twofold: to improve the spatiotemporal resolution and SNR so as to achieve a faithful readout of channel gating kinetics and localization; and to develop imaging techniques sufficiently simple and reproducible to complement and, for some purposes perhaps supplant, electrophysiological techniques for single-channel recording.

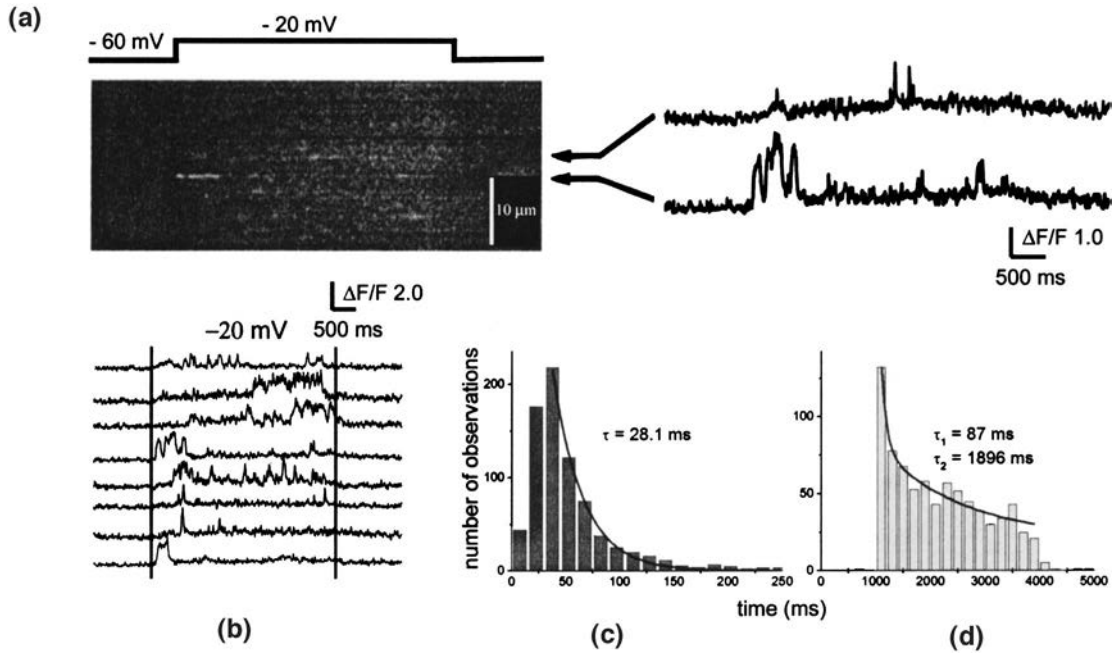

Fig. 2 Single-channel fluorescence signals recorded by linescan confocal imaging in oocytes loaded with fluo-4-dextran. (a) Linescan confocal image shows fluorescence Ca^{2+} signals evoked by a depolarizing step from −60 to −20 mV. Distance along the 50-μm scan line is depicted vertically in the image, time runs from left to right, and increasing fluorescence ratios (corresponding to increasing free $[Ca^{2+}]$ are depicted by increasingly lighter shades. Bars indicate the duration of the step and traces indicate measurement of local (3 pixels average) fluorescence from two regions marked by the arrows. (b) to (d) Sparklet kinetics during depolarizations to −20 mV: (b) sample traces showing sparklets evoked at 6 sites along a line scan in response to depolarization to −20 mV, delivered when indicated by the vertical bars; (c) distribution of sparklet life times (measured at half-maximal amplitude); and (d) occurrence of sparklets at different times during depolarizing pulses, showing bi-phasic inactivation kinetics. Data are reproduced from Ref. 9.

2 Optical Single-Channel Recording

We describe the use of two imaging modalities to monitor single-channel Ca^{2+} flux. We began by using confocal microscopy, which monitors fluorescence from a diffraction-limited confocal spot with dimensions of roughly 300 nm in the lateral plane and 800 nm axially, and can thus provide a readout from a subfemtoliter volume of cytoplasm around a channel [Fig. 1(a, inset)]. However, a limitation is that confocal images must be constructed point by point by scanning a laser spot through the specimen. The maximum scan speed is limited by mechanical constraints, and raster scanning of 2-D *x*-*y* images has not been practicable at the rates required to resolve channel gating kinetics (although developments with spinning-disk confocal microscopes may obviate this limitation). Instead, we[9] and others[8] used a linescan mode, whereby the confocal spot is repeatedly scanned along a single line to achieve a temporal resolution as high as 1 ms per line [Fig. 1(a)]. Drawbacks of this approach are that it gives spatial information in only one dimension, samples relatively few channels at a time, and introduces uncertainty in interpreting records because Ca^{2+} may diffuse from channels some distance from the scan line. We thus went on to explore the use of TIRFM [Fig. 1(b)], which, as described below, provides a 2-D image of Ca^{2+} signals from a very thin (ca. 100-nm) optical ''section'' of the cytoplasm immediately adjacent to the plasma membrane [Fig. 1(b, inset)]. TIRFM thus has the ability to simultaneously monitor highly localized signals from hundreds of channels,[10] but, unlike confocal microscopy, its use is restricted to plasma membrane channels as the optical section cannot be focused into the cell to record activity of channels in intracellular membranes.

2.1 *Confocal Laser Scan Microscopy*

We used *Xenopus* oocyte as a model cell system to image Ca^{2+} flux through channels expressed by $\alpha_{1B\text{-}d}$ and β_3 subunits of an *N*-type voltage-gated Ca^{2+} channel.[19] Depolarization of the oocyte membrane produced localized, stepwise transients in linescan images, which we interpret to arise from Ca^{2+} flux through single channels. Following the nomenclature introduced by Wang et al. to describe signals from voltage-gated *L*-type channels,[8] we refer to these as ''sparklets.'' Figure 2(a) shows a linescan image of sparklets arising autonomously at localized sites in response to a weak (−20 mV) depolarizing pulse that gave a low probability of channel opening. Several observations indicate that these fluorescence signals arose owing to Ca^{2+} entry through individual expressed *N*-type channels:[9] (1) no signals were observed in control (non-messenger ribonucleic acid (mRNA)-injected) oocytes; (2) responses became smaller when extracellular $[Ca^{2+}]$ was lowered from 6 to 1.8 mM; (3) signals were abolished by 2 μM extracellular Ni^{2+}, a selective blocker of voltage-gated Ca^{2+} channels; (4) the frequency of sparklets increased progressively at potentials positive to about −25 mV, mirroring the voltage-dependent activation of *N*-type channels,[17] and their amplitudes reduced to zero at voltages near the Ca^{2+} equilibrium potential; (5) signals were of uni-

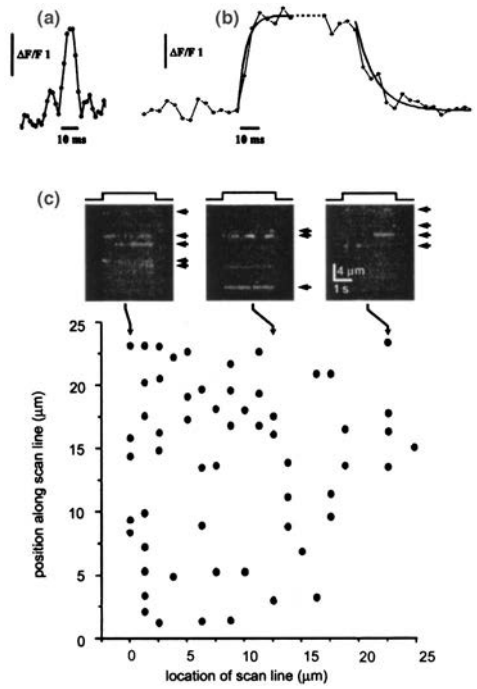

Fig. 3 Temporal and spatial resolution of sparklets imaged by confocal microscopy. (a) and (b) Temporal resolution of sparklets imaged at a scan rate of 2 ms/line: (a) a single, brief sparklet and (b) average of nine longer sparklets formed after aligning their rising phases (left) and falling phases (right). Exponential curves fitted to the rising and falling phases have respective time constants of 4 and 10 ms. Note the slower falling phase as compared to the brief event in (a), resulting from local Ca^{2+} accumulation during the longer channel openings. (c) Two-dimensional map of channel locations, constructed by locating the vertical positions of sparklets along the scan line in response to depolarizing pulses (arrows next to linescan images) while moving the scan line in horizontal increments of 1.25 μm in the horizontal axis. Data are reproduced from Ref. 9.

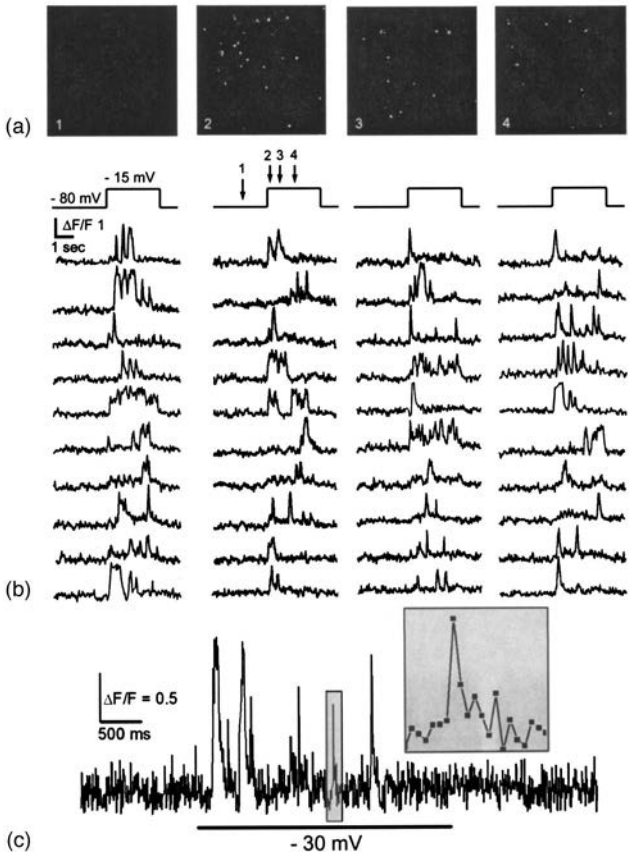

Fig. 4 Two-dimensional imaging of sparklets by TIRFM: (a) Sequence of individual video frames of TIRFM images showing sparklets arising at several sites throughout the image field during a depolarizing pulse (to −15 mV) to activate *N*-type Ca^{2+} channels expressed in the oocyte membrane and (b) Traces show local (0.7×0.7-μm) fluorescence signals recorded independently and simultaneously at a frame rate of 30 s^{-1} from over 40 channels during a single depolarizing pulse. Numbered arrows mark times during the depolarizing pulse when the respective images in (a) were captured. (c) Improved kinetic resolution of sparklets obtained using a camera (Cascade, Roper Scientific) operated at 200 frames s^{-1}. The main trace shows fluorescence recorded from a single sparklet site in response to a 3-s depolarizing pulse to −30 mV, and the inset shows an expanded view of a selected event (boxed in gray). Data in (a) and (b) are reproduced from Ref. 10.

tary amplitude, and displayed pulsatile, random kinetics consistent with Markovian gating of single channels; and (6) the signal mass of the fluorescence transients was consistent with the expected single-channel Ca^{2+} current.

We analyzed several hundred sparklets evoked by depolarization to −20 mV [Fig. 2(b)]. Event durations followed a single exponential with a time constant of about 28 ms [Fig. 2(c)], and the frequency of sparklets declined throughout the pulse following a double exponential [Fig. 2(d)], reflecting the inactivation kinetics of the channels. Sparklet durations are, in principle, expected to follow a continuous exponential distribution, reflecting the underlying stochastic variation in open lifetimes of the Ca^{2+} channels. The fall-off in observations with durations <20 ms is likely, therefore, to reflect a failure to resolve fluorescence signals arising from brief channel openings. Factors contributing to this filtering likely included both the relatively slow (4 ms/line) scan rate and inclusion of nonfocal events. By using faster scan rates (2 ms/line) we could resolve ''square'' events with durations <10 ms, and rise and fall times of ~4 ms [Fig. 3(a)]. Although brief events showed roughly symmetrical rise and fall times, the decay of fluorescence at the end of longer sparklets was slower than the rise [respective time constants about 4 and 10 ms: Fig. 3(b)], and slower than following brief sparklets [e.g., Fig. 3(a)], probably because the greater accumulation of Ca^{2+} around the channel was slower to dissipate. This latter factor also introduced a further distortion in that the basal fluorescence showed a slow rise throughout several hundred ms during bursts of sparklets.

Macroscopic Ca^{2+} signals evoked by strong depolarizations revealed a ''patchy'' spatial distribution, with functional *N*-type Ca^{2+} channels concentrated within regions a few tens of micrometers across, while neighboring regions of the membrane appeared almost devoid of channels. To demonstrate the capability for submicrometer mapping of individual channels, we selected a low-density region and applied strong depolarizations expected to open almost all channels at least once during each trial. The coordinates of channels along the scan line were located by identifying the positions of sparklets in

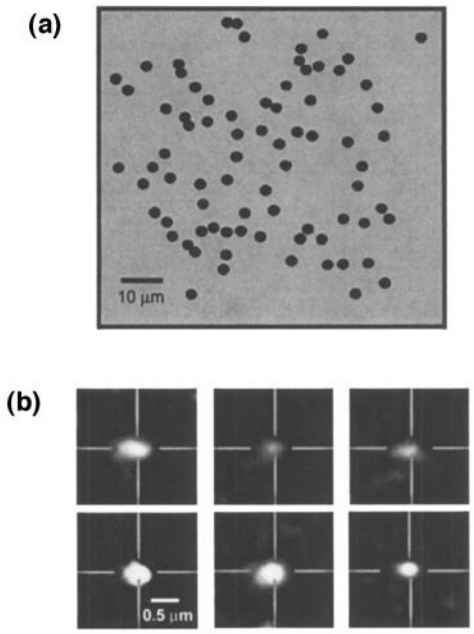

Fig. 5 Spatial mapping and tracking of *N*-type Ca^{2+} channels by TIRFM: (a) Map showing channel locations within an 80×80-μm^2 patch of the oocyte membrane, constructed by marking the positions of all sparklets observed during 10 successive depolarizing pulses, and (b) *N*-type channels immobile in the oocyte membrane. Images show sparklets evoked at a fixed location in the membrane in response to successive depolarizing pulses delivered over a period of 5 min. Crosshairs mark the centroid of the first sparklet.

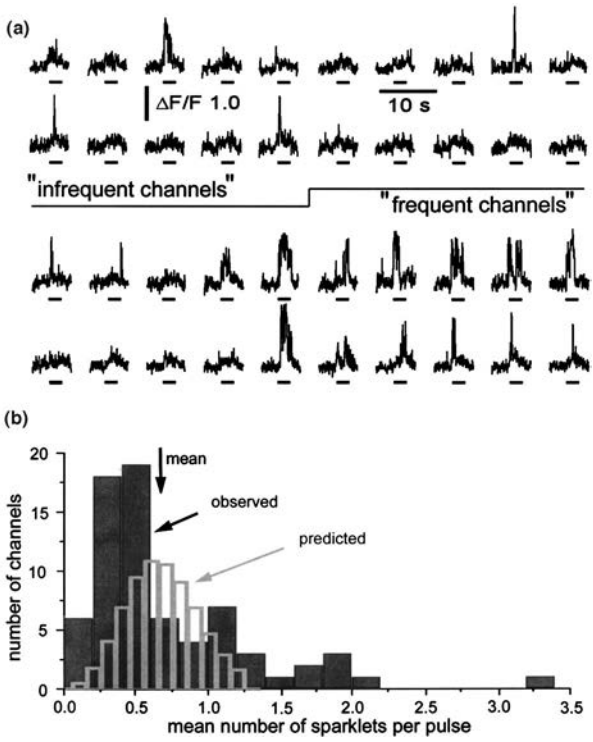

Fig. 6 TIRFM imaging reveals that adjacent *N*-type channels display markedly different gating kinetics: (a) Representative local fluorescence traces illustrating two channels that showed infrequent sparklets (upper) and two channels that showed frequent sparklets (lower), each row of traces shows records obtained at a single site in response to 10 successive depolarizing pulses, and (b) Solid histogram bars show the observed distribution of mean sparklet frequencies (mean number of sparklets evoked at each site during 10 successive depolarizations) measured from 72 channels within a 60×60-μm region of membrane. Open bars indicate the expected distribution if sparklet frequencies followed a Poisson distribution with the same overall mean (0.68 sparklets/pulse) as the experimental data. Data are reproduced from Ref. 10.

linescan images [marked by arrowhead by images in Fig. 3(c)]. This procedure was then repeated as the scan line was stepped in increments of 1.25 μm along the orthogonal axis, so as to build up a 2-D map of channel locations within a 25×25-μm region of the oocyte membrane [Fig. 3(c)].

2.2 *TIRFM*

We next explored the use of TIRFM for rapid 2-D imaging of cytosolic Ca^{2+} signals arising very close to the cell membrane.[10] TIRFM works by directing excitation light through a glass substrate toward an aqueous specimen at a sufficiently shallow angle that total internal reflection (TIR) occurs due to the refractive index decrease at the glass/water interface. However, a very thin electromagnetic field (evanescent wave) is created in the liquid with the same wavelength as the incident light, and decays exponentially with distance from the interface (typically over one or a few hundred nanometers). Because this field is able to excite fluorophores near the interface while avoiding excitation further into the aqueous phase it provides an ''optical sectioning'' effect similar to but even narrower than that achieved by a confocal microscope.[20] Moreover, TIRFM provides uniform illumination throughout a 2-D plane so that, because there is no need to scan a laser spot, the imaging speed is limited only by the frame rate of the camera or by shot-noise considerations. Although the idea of TIRFM is old, its biological utility has expanded greatly recently with the development of specialized oil-immersion objective lenses[20] having very high NAs (1.45 or greater). These enable the excitation light to be directed to the specimen at a shallow angle through the very edge of the lens while using a high-sensitivity CCD camera to visualize fluorescence in the evanescent field through the same objective [Fig. 1(b)].

We again used the expression of voltage-gated Ca^{2+} channels in *Xenopus* oocytes as a model system to demonstrate single-channel Ca^{2+} imaging.[10] To achieve TIRF conditions it was first necessary to strip away the vitelline envelope that normally surrounds the oocyte. These ''naked'' oocytes adhered sufficiently close to a cover slip to bring the cell membrane and immediately adjacent cytoplasm within the evanescent field, with only a thin intervening film of extracellular solution. Depolarizing pulses applied via a two-electrode voltage clamp then evoked numerous highly localized and transient flashes of fluorescence [''sparklets'': Fig. 4(a)] throughout the image field (60×60 μm of membrane). In line with confocal imaging data already presented, we associated the sparklets with the openings of single *N*-type channels. Fluorescence measurements from small regions of interest centered on sparklets showed stochastic pulsatile signals [Fig.

Table 1 Single-channel recording: comparison of the patch-clamp technique with various optical imaging modalities—wide-field fluorescence (WFFM), confocal linescan (CLSM), and TIRFM.

		Optical Recording		
	Cell-Attached Patch Clamp	WFFM	CLSM	TIRFM
Cytoskeletal disruption	Likely, owing to giga-seal formation	None	None	Probably minimal
Spatial information	Coarse—possible only by repeated patching	Submicrometer resolution but only for low channel density	Submicrometer resolution in one dimension	Excellent: 2-D submicrometer resolution of densely packed channels
Temporal resolution	Submillisecond	A few tens of milliseconds	A few milliseconds	A few milliseconds
Independent channels monitored	One per patch	Limited to low channels density (few channels/cell)	Simultaneous detection of 10 to 20 channels	Simultaneous detection of >300 channels: (density >0.1 channel/μm^2)
Ionic permeability	No restriction	Requires channels with at least some Ca^{2+} permeability	Requires channels with at least some Ca^{2+} permeability	Requires channels with at least some Ca^{2+} permeability
Channel motility	Channel constrained within patch by giga-seal	Can track channel position in areas with low channel density	Difficult to track channel motility as only one spatial dimension	Can track channel position with submicrometer resolution

4(b)] that look remarkably like patch-clamp recordings. Our initial experiments[10] were done using a camera with a frame rate of only 30 s^{-1}, but we have subsequently obtained a much improved time resolution (sparklets with durations of ca. 5 ms) using a faster camera [Fig. 4(c)].

TIRFM imaging readily enabled rapid 2-D mapping of channels in the membrane by locating the positions of sparklets evoked during depolarizing pulses [Fig. 5(a)]. Moreover, the location of individual sparklets could be tracked over periods of several minutes with submicrometer resolution, revealing that *N*-type channels expressed in the oocyte membrane appear to be rigidly anchored [Fig. 5(b)]. Finally, the ability to record simultaneously and independently from many channels enabled comparison of the gating kinetics of channels within a given region of the membrane. We observed a considerable variation in sparklet frequency between closely located channels, with many showing one or two events and fewer showing up to 20 sparklets throughout 10 consecutive depolarizing pulses [Fig. 6(a)]. The experimental data differ appreciably from the Poisson distribution predicted if the channels displayed a probability equal to the population mean [Fig. 6(b)]. Thus, substantial channel-to-channel variation in open probability exists even between nominally identical and closely adjacent channels, possibly reflecting differences in channel gating mode.

3 Discussion

Single-channel imaging promises several advantages over patch-clamp techniques for studying ion channel function. Most notably, simultaneous records can be obtained independently from tens or hundreds of channels, whereas measurements of currents from multiple channels within a membrane patch cannot readily be disentangled. Moreover, imaging provides information that electrophysiological measures cannot. For example, channel locations can be mapped with submicrometer precision, their motility (or lack of it) can be followed over time, and simultaneous comparisons between closely adjacent and nominally identical channels reveal marked differences in gating kinetics.

A further advantage is that optical imaging provides an inherent amplification that is absent with electrophysiological techniques. Each Ca^{2+} ion contributes only two electron charges to a patch-clamp recording, whereas a fluorophore probe molecule can be excited to emit hundreds or thousands of photons per millisecond after binding a single Ca^{2+} ion. Thus, fluorescence signals with good signal-to-noise ratio can be obtained by imaging Ca^{2+} flux through *N*-type channels with relatively physiological ionic compositions (extracellular $[Ca^{2+}] = 6$ mM), whereas patch-clamp recordings typically utilize high concentrations of Ba^{2+} to produce currents large enough to resolve. There is a limitation, however, as to which ions can be optically sensed, and Ca^{2+} ions are at present the only species for which detection at a single-channel level is feasible. In part, this is because of the availability of highly sensitive and selective fluorescent Ca^{2+} indicators,[21] but more importantly because of the enormous changes in Ca^{2+} concentration that occur near the mouth of an open Ca^{2+} channel. Since the resting cytosolic $[Ca^{2+}]$ is maintained at a few tens of nanomolar the local concentration can increase a thousandfold when a Ca^{2+}-permeable channel opens, whereas corresponding changes for ions such as Na^+ or Cl^- are less than 10-fold. It seems unlikely, therefore, that a similar approach

would be feasible to monitor, for example, the flux of Cl^- ions through gamma-aminobutric acid (GABA)-activated inhibitory channels. Nevertheless, numerous diverse channels show appreciable Ca^{2+} permeability and are potential targets for single-channel Ca^{2+} imaging even though they are not primarily thought of as Ca^{2+} channels. For example, we have been able to image Ca^{2+} flux through muscle nicotinic receptors expressed in the oocyte membrane.

Table 1 summarizes some of the relative advantages and limitations of various optical single channel recording techniques versus patch clamp recording. Patch clamping is likely to retain advantages in several important aspects, including superior temporal resolution, measurement of absolute current magnitudes, ability to record currents carried by any ionic species and its built in control of membrane voltage. However, it has limitations including lack of spatial information, readout from only one channel at a time, the necessity of physical access of the pipette to the membrane, and possible disruption of the cytoskeleton and channel function during giga-seal formation. For these reasons, we believe that optical imaging will evolve as a powerful adjunct to the patch-clamp technique, as these methodologies have complementary advantages. Imaging is inherently less invasive, can simultaneously monitor numerous channels, and provides a powerful methodology for investigating ion channel distribution and motility within the cell membrane.

Among the different optical imaging modalities, the derivation of signal mass from wide-field images[6,7,15] is presently the most accurate way to quantify the magnitude of Ca^{2+} current through a single channel, but wide-field imaging otherwise provides less than optimal temporal resolution and is restricted to sparsely distributed channels. Optical sectioning techniques such as confocal and TIRFM are substantially better in the latter respects. Confocal microscopy has the advantage that it can image signals arising from Ca^{2+}-release channels deep within a cell,[11–14] but to achieve sufficient temporal resolution it has thus far been used only in linescan mode where spatial information is restricted to a single dimension. Overall, we believe that TIRFM is the imaging modality of choice for studying channels in the plasma membrane of cells that can be made to adhere closely to a cover glass. It enables simultaneous 2-D imaging of numerous channels (our present record is >300 channels within a 40×40-μm membrane area), and can provide a time resolution of a few milliseconds when used in conjunction with a camera having a sufficiently fast frame rate. Although there are concerns regarding the restricted extracellular fluid space between the cover slip and membrane, in practice we have not found this to be a problem. In particular, sparklet amplitudes show little or no ''run down'' as might be expected if there were appreciable depletion of Ca^{2+} in the local extracellular space, and channel-blocking drugs and agonists exchange within a few tens of seconds with the bulk bathing solution.[22] Finally, we note that TIRFM is relatively simple and inexpensive to implement, such that an existing fast Ca^{2+}-imaging system could be adapted simply by the addition of a commercially available TIRF illuminator and specialized objective lens. In addition to applications in basic research, single-channel imaging holds promise for high-throughput screening of ion channel activity, and may be more easily implemented than efforts to develop massively parallel arrays of patch-clamp electrodes.[23,24]

Acknowledgments

We thank Diane Lipscombe for a kind gift of *N*-type Ca^{2+} channel clones. This work was supported by Grants GM48071 and GM65830 from the National Institutes of Health.

References

1. E. Neher and B. Sakmann, ''Single-channel currents recorded from membrane of denervated frog muscle fibres,'' *Nature (London)* **260**, 799–802 (1976).
2. O. P. Hamill, A. Marty, E. Neher, B. Sakmann, and F. J. Sigworth, ''Improved patch-clamp techniques for high-resolution current recording from cells and cell-free membrane patches,'' *Pflugers Arch.* **391**, 85–100 (1981).
3. R. Iino, I. Koyama, and A. Kusumi, ''Single molecule imaging of green fluorescent proteins in living cells: E-cadherin forms oligomers on the free cell surface,'' *Biophys. J.* **80**, 2667–2677 (2001).
4. M. J. Schnitzer, K. Visscher, and S. M. Block, ''Force production by single kinesin motors,'' *Nat. Cell Biol.* **10**, 718–723 (2000).
5. A. Sonnleitner, L. M. Mannuzzu, S. E. Terakawa, and Y. Isacoff, ''Structural rearrangements in single ion channels detected optically in living cells,'' *Proc. Natl. Acad. Sci. U.S.A.* **99**, 12759–12764 (2002).
6. H. Zou, L. M. Lifshitz, R. A. Tuft, K. E. Fogarty, and J. J. Singer, ''Imaging Ca^{2+} entering the cytoplasm through a single opening of a plasma membrane cation channel,'' *J. Gen. Physiol.* **114**, 575–588 (1999).
7. H. Zou, L. M. Lifshitz, R. A. Tuft, K. E. Fogarty, and J. J. Singer, ''Visualization of Ca^{2+} entry through single stretch-activated cation channels,'' *Proc. Natl. Acad. Sci. U.S.A.* **99**, 6404–6409 (2002).
8. S. Q. Wang, L. S. Song, E. G. Lakatta, and H. Cheng, ''Ca^{2+} signalling between single L-type Ca^{2+} channels and ryanodine receptors in heart cells,'' *Nature (London)* **410**, 592–596 (2001).
9. A. Demuro and I. Parker, ''Optical single channel recording: imaging Ca^{2+} flux through individual N-type voltage-gated chanels expressed in *Xenopus* oocytes,'' *Cell Calcium* **34**, 499–509 (2003).
10. A. Demuro and I. Parker, ''Imaging the activity and localization of single voltage-gated Ca^{2+} channels by total internal reflection fluorescence microscopy,'' *Biophys. J.* **86**, 3250–3259 (2004).
11. H. Cheng, W. J. Lederer, and M. B. Cannell, ''Calcium sparks: elementary events underlying excitation-contraction coupling in heart muscle,'' *Science* **262**, 740–744 (1993).
12. M. Bootman, E. Niggli, M. Berridge, and P. Lipp, ''Imaging the hierarchical Ca^{2+} signaling system in HeLa cells,'' *J. Physiol. (London)* **499**, 307–314 (1997).
13. I. Parker and Y. Yao, ''Ca^{2+} transients associated with openings of inositol trisphosphate-gated channels in *Xenopus* oocytes,'' *J. Physiol. (London)* **491**, 663–668 (1996).
14. P. Lipp and E. Niggli, ''Submicroscopic calcium signals as fundamental events of excitation—contraction coupling in guinea-pig cardiac myocytes,'' *J. Physiol. (London)* **492**, 31–38 (1996).
15. H. Zou, L. M. Lifshitz, R. A. Tuft, K. E. Fogarty, and J. J. Singer, ''Imaging calcium entering the cytosol through a single opening of plasma membrane ion channels: SCCaFTs—fundamental calcium events,'' *Cell Calcium* **35**, 523–533 (2004).
16. X.-P. Sun, N. Callamaras, J. S. Marchant, and I. Parker, ''A continuum of $InsP_3$-mediated elementary Ca^{2+} signalling events in *Xenopus* oocytes,'' *J. Physiol. (London)* **509**, 67–80 (1998).
17. M. Naraghi and E. Neher, ''Linearized buffered Ca^{2+} diffusion in microdomains and its implications for calculation of $[Ca^{2+}]$ at the mouth of a calcium channel,'' *J. Neurosci.* **17**, 6961–6973 (1997).
18. E. Rios and M. D. Stern, ''Calcium in close quarters: microdomain feedback in excitation-contraction coupling and other cell biological phenomena,'' *Annu. Rev. Biophys. Biomol. Struct.* **26**, 47–82 (1997).
19. Z. Lin, S. Haus, J. Edgerton, and D. Lipscombe, ''Identification of functionally distinct isoforms of the N-type Ca^{2+} channel in rat sympathetic ganglia and brain,'' *Neuron* **18**, 153–166 (1997).
20. D. Axelrod, ''Total internal reflection microscopy in cell biology,'' *Methods Enzymol.* **361**, 1–33 (2003).
21. A. Minta, J. P. Kao, and R. Y. Tsien, ''Fluorescent indicators for

cytosolic calcium based on rhodamine and fluorescein chromophores,'' *J. Biol. Chem.* **264**, 8171–8178 (1989).
22. I. Parker and A. Demuro, unpublished data.
23. F. J. Sigworth and K. G. Klemic, ''Patch clamp on a chip,'' *Biophys. J.* **82**, 2831–2832 (2002).
24. J. Xu, X. B. Wang, B. Ensign, M. Li, L. Wu, A. Guia, and J. Xu, ''Ion-channel assay technologies: quo vadis?'' *Drug Disc. Today* **6**, 1278–1287 (2001).